

Synthesis, Characterization, and Anticancer Activities of Zn²⁺, Co²⁺, and Ni²⁺ Complexes Containing Aza Hetero Ligands

Amir Nazeer¹, Qasim Umar², Zhang Li¹, Yanting Yang¹, Mei Luo^{1*}

¹Department of Chemistry and Chemical Engineering, Hefei University of Technology, Hefei, 23000, P.R. China

²Department of Chemistry, University of Science and Technology of China, 96 Jinghai Road, Hefei, 230026,

*Corresponding author: Mei Luo. Department of Chemistry and Chemical Engineering, Hefei University of Technology, Hefei, 23000, P.R. China. Email: luomei@pku.edu.cn

Citation: Nazeer A, Umar Q, Li Z, Yang Y, Luo M (2024) Synthesis, Characterization, and Anticancer Activities of Zn²⁺, Co²⁺, and Ni²⁺ Complexes Containing Aza Hetero Ligands. Annal Cas Rep Rev: ACRR-382.

Received Date: 18 March, 2024; **Accepted Date:** 21 March, 2024; **Published Date:** 26 March, 2024

Abstract

With numerous uses in synthesis and therapeutics, aza-heterocyclic ligands are an exciting class of coordination chemicals. Three Zn(II), Co(II), and Ni(II) complexes (I-III) such as [ZnC₁₆H₁₆N₆O₁₂] (I), [CoC₁₆H₁₆N₆O₁₂] (II), and [Ni₂C₃₄H₃₈N₆O₁₁] (III) bearing aza-heterocyclic ligands have been synthesized under one-pot self-assembly conditions. The reaction of 2,3-dihydroxyquinoxaline with Zn(NO₃)₂•6H₂O and Co(NO₃)₂•6H₂O respectively, produced two mononuclear complexes (I) and (II) while the binuclear complexes (III) were synthesized using NiCl₂•6H₂O, with salicylidene salicylhydrazide. Then, the complexes were characterized using MS, FT-IR UV-Vis, and X-ray diffraction to confirm their structures. The synthesized complexes were employed against different human tumor cell lines (SMMC-7721, A549, MDA-MB-231, and SW480). Complex (III) exhibited the best activity against human tumor cell lines MDA-MB-231, which are late-stage breast cancer cells, with an IC₅₀ value of 6.57 μM.

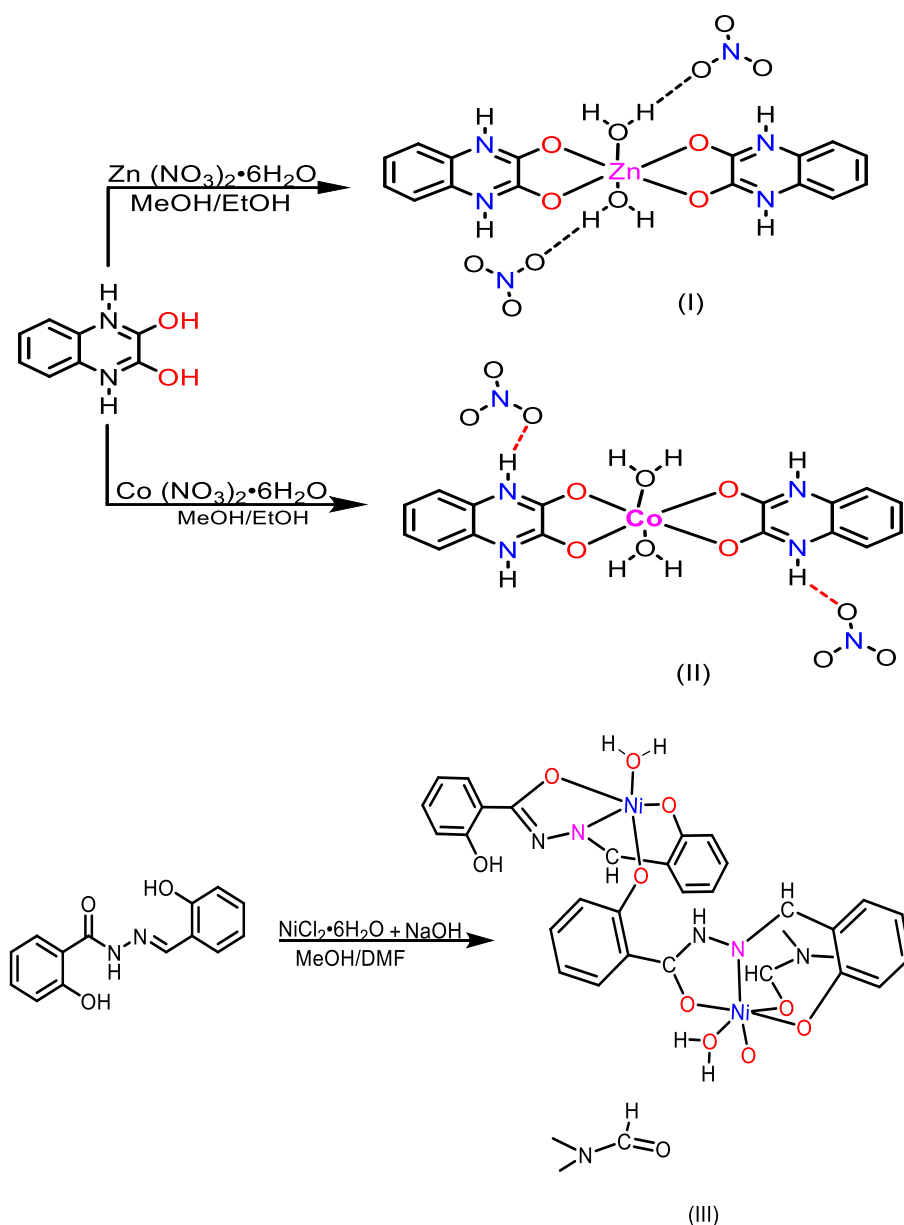
Keywords: Aza heteroatom ligands, Metal complexes, Crystal structure, Toxicity.

Introduction

Transition metal complexes, which comprise organic ligands linked to the central metal, have been recognized for their usefulness in various areas, including modern research, medicinal drug synthesis (e.g., anti-cholesterol, anti-HIV, antibacterial, antifungal, analgesic, and anti-cancer), and the development of humanity [1–12]. Organometallic complexes involving N-containing heterocyclic molecules are of significant interest across various fields [13,14] They act as vital organic intermediates in pharmaco-chemistry and organic synthesis [15]. Abdolmaleki et al. (2022) synthesized Ni²⁺ complexes of 2,6-pyridine dicarboxylate, which exhibit promising potential as an anticancer agent, with an IC₅₀ value of 5.13 μM [16]. Gangu et al. (2017) synthesized coordination complexes using 4,5-imidazole dicarboxylic acid as organic ligands. These complexes exhibited notable catalytic activity for environmentally safe chemical transformations, following ecological principles [17]. It is widely accepted that copper complexes have medicinal and catalytic uses. In 2016, Swamy et al. synthesized Cu (II) complex, which was the result of combining imidazole and 2,6-pyridine dicarboxylic acid; in vitro, it exhibited greater antibacterial activity than the respective ligand [18]. In 2014, a novel mixed-ligand binuclear

Co²⁺ complex was synthesized by Nfor et al. The complex's magnetic susceptibility measurements indicate the presence of antiferromagnetic interactions among the Co²⁺ ions contained within the dinuclear units [19]. Salama, Ahmed, and Hassan in 2017, synthesized and studied Co²⁺ complexes of amino acid Schiff bases from salicylaldehyde and three amino acids in a basic medium, and also studied their biological activities [20]. Recently, there has been a surge in interest surrounding coordination molecules composed of nitrogen heteroatoms and the initial transitional metals, owing to their efficacy against cancer and their low level of toxicity [21–23].

In this research work, three new compounds were synthesized according to the previously published work using a one-pot synthesis technique [24]. [ZnC₁₆H₁₆N₆O₁₂] (I), [CoC₁₆H₁₆N₆O₁₂] (II), and [Ni₂C₃₄H₃₈N₆O₁₁] (III), which were identified using techniques such as UV-vis spectroscopy, FT-IR, and single-crystal X-ray diffraction. Presently, cancer stands as the most severe disease, and researchers are tirelessly working to develop therapeutic medicines. Our synthetic complexes exhibit admirable cytotoxicity towards different human tumor cell lines (SMMC-7721, A549, MDA-MB-231, and SW480), but negligible toxicity to normal cells.



Scheme 1:^(I)Synthetic scheme for complex (I), ^(II)Synthetic scheme for complex (II), ^(III)Synthetic scheme for complex (III).

Experimental

Materials and Methods

The reagents and raw materials were utilized in their original state without undergoing any purification or processing. 2,3-dihydroxyquinoxaline, and salicylidene salicylhydrazide, were purchased from J&K Scientific LTD. Metal salts Zn(NO₃)₂·6H₂O, Co(NO₃)₂·6H₂O, and NiCl₂·6H₂O were bought from Acros while solvents such as methanol and ethanol, DMF and H₂O were purchased from Sinopharm Chemical Reagent Company. The solvent used in combination with tetramethylsilane (TMS) was used as an internal standard, and chemical shifts were recorded in ppm (δ) (residual CHCl₃, H 7.26 ppm; CDCl₃, C, 77 ppm). Multiples are denoted by the abbreviations s = singlet, d = doublet, t = triplet, and m = multiplet. In cm⁻¹, the peaks are reported for infrared spectra taken with a Mattson Galaxy Series FTIR 3000 spectrometer. A Gemini S Ultra diffractometer was used to determine the crystal structure. Elemental analysis was carried out on an AE-3000 (Elemental Analyser). The Yanaco Micro melting point system MP-J3 and the SYNSYO melting point apparatus SMP-500

were used to measure the melting point, and they were not adjusted.

Cytotoxicity assay

In the cytotoxic investigation, human tumor cell lines (SMMC-7721, A549, MDA-MB-231, and SW480) were utilized. The cells were acquired from the ATCC in (Manassas, Virginia, USA). Cells were grown in RPMI-1640 or DMEM (Biological Industries, Kibbutz Beit Haemek, and Israel) at 37 °C in a humid environment with 5% CO₂ and with 10% foetal bovine serum added (Biological Industries). The cytotoxicity experiment was analyzed using an MTS (Promega, Madison, WI, USA) assay. The 3-(4,5-dimethylthiazol-2-yl)-5-(3-carboxymethoxyphenyl)-2-(4-sulfophenyl)-2H-tetrazolium, inner salt (MTS) assay (Promega, Madison, WI, USA) was used to evaluate the cytotoxicity assay. The cells were seeded into each well of a 96-well cell culture plate. The test reagent (100 M) was added at 37 °C after 12 h of incubation. After the cells were incubating for 48 hours at 37 °C, the MTS test was performed. Compound AH106 was rescreened at concentrations of 100, 50, 25, 12.5, and 6.25 M while the remaining compounds were rescreened at

concentrations of 200, 100, 50, 25, and 12.5 M using cisplatin and paclitaxel (Sigma, St. Louis, MO, USA) as positive controls. Compounds at these concentrations that exhibited a 50% growth inhibition rate were further investigated. Using Reed and Muench's approach, the IC₅₀ value of each chemical was determined. The findings are provided in (Table 4).

General Experimental Details

Clean and dried glassware was used under normal pressure for all reactions. Reagents were purchased from commercial sources. The temperature was controlled by 'ZNCL-TS Intelligent Magnetic Stirrer' and used a condenser to control evaporation. A Bruker 500 MHz Advance III Spectrometer was used to collect nuclear magnetic resonance (NMR) spectra. To obtain infrared spectra, an FTIR 3000 spectrometer from the Mattson Galaxy Series was used, and peak values were recorded in cm⁻¹. E. A was carried out on VARIO ELIII elemental analyzer. A Gemini S Ultra Diffractometer was used to determine the crystal structure. Chemical shifts of ¹H were recorded in ppm and referenced to DMSO-*daa* 6, 2.50 ppm; for CDCl₃, 7.26 ppm. s = singlet, d = doublet, t = triplet, and m = multiplet were used as the shorthand letters to indicate different multiplicities. Both the Yanaco Micro Melting Point System MP-J3 and the SANSYO Melting Point Apparatus SMP-500 were utilized to make accurate measurements of melting points.

General procedure for the syntheses of complexes (I)-(III)

The mixture of ligand and metal salt was heated from and refluxed in a 100 mL round bottom flask. The temperature was controlled by 'ZNCL-TS Intelligent Magnetic Stirrer' and a condenser was used to control evaporation. Rapid filtering occurred after the reaction, and the filtrate was obtained for steady volatilization. Complexes containing Zn⁺², Co⁺², and Ni⁺² were successfully synthesized by reacting 2,3 dihydroxyquinoxaline, and salicylidene salicylhydrazide as ligands with Zn (NO₃)₂•6H₂O, Co (NO₃)₂•6H₂O, and NiCl₂•6H₂O, respectively. X-ray diffraction, FTIR, UV, MS, and E.A. were used to examine and characterize the synthesized crystals. The first key was to find the appropriate ligands. After this, reacting the ligands with the proper metal salts yields the filtrate or residue from the reaction, which is then analyzed to determine which solvent is effective for crystal precipitation. Tetrahydrofuran (THF), anhydrous methanol, ethanol, and chloroform are the accessible solvents needed for this stage and are the most important. Crystals can be stored in a refrigerator if these substances cannot precipitate at room temperature.

Synthesis of the complexes (I-III)

(Complex I) Using general procedure (molar ratio 1:5) 2,3 dihydroxyquinoxaline 2.7 mmol (0.44 g) and methanol anhydrous 25 mL was put into 100 mL round bottom flask, 25 mL ethanol was added after 5 minutes to this solution, 4.01 g (13.5 mmol) of Zn (NO₃)₂•6H₂O was added. At 80 °C, the mixture was stirred for 24 hours. Following the completion of the reaction, the hot solution was filtered into a 50 mL beaker. After being put in a beaker sealed in plastic wrap which was punctured with a small needle, the solvent evaporated naturally

at room temperature within three days, forming white crystals, m.p. 115 °C, single-crystal X-ray analysis was possible with this data. The yield was 80% (0.352 g). IR (KBr, n, cm⁻¹): 3370, 3221 (–NH), 2955 (=C–H), 1654 (–NO₃), 1601, (–C=C–), 1312 (C–N), 1042 (C–O), 647 (–Zn–O). HRMS(m/e) Cal: 549.72 found: 549.0492.

(Complex II) In accordance with the general procedure (molar ratio 1:5), the synthetic method of complex (II) is the same as for complex (I), the only difference is metal salt. 25 mL methanol anhydrous and 2,3 dihydroxyquinoxaline 3.2 mmol (0.53 g) were put into a 100 mL round bottom flask. After a few minutes, 25 mL ethanol was added, and then 4.67 g (16.0 mmol) of Co (NO₃)₂•6H₂O was added. The reaction was refluxed for 24 hours at 80 °C. The hot solution was passed into a 50 mL beaker after the reaction. The liquid evaporated naturally at room temperature for three days After being put in a beaker sealed with plastic wrap which was perforated with a small needle. It formed brownish crystals with a melting point of 120 °C. These crystals could be used for single-crystal X-ray analysis. The yield was 78% (0.414 g). IR (KBr, n, cm⁻¹): 3337, 3228 (–NH), 2960 (=C–H), 2321 (–CH), 1643 (–NO₃), 1615, (–C=C–), 1320 (C–N), 895 (C–O), 622 (–Co–O). HRMS(m/e) Cal: 543.28 found: (M+H)544.033.

(Complex III) Using general procedure (molar ratio 1:1), complex (III) was synthesized and characterized using a salicylidene salicylhydrazide 2.34 mmol (0.6 g), and 30 mL methanol anhydrous was put into a 100 mL round bottom flask, 20 mL DMF was added after 5 minutes to this solution, NiCl₂•6H₂O 2.34 mmol (5.56 g) was added. NaOH 1.5 mmol (0.06 g) was added (dissolved in 15ml H₂O) after 5 minutes of refluxing at 90 °C, the purpose of adding a strong base to the reaction was to activate the active sites, the mixture was then stirred for 36 hours. Following the completion of the reaction, the hot solution was filtered into a 50 mL beaker. The solvent naturally evaporated at room temperature after 7 days of covering the beaker with plastic wrap and making pores in it with a small needle, yielding dark green crystals, The yield was 83% (0.498 g). m.p. 155 °C, single-crystal X-ray analysis was possible with the abovementioned data. IR (KBr, n, cm⁻¹): 3728 (–OH), 3333 (–NH), 2928 (=C–H), 1664 (–C=C–), 1517, (–C=C), 1463 (C=C), 1403 (C–C), 953 (C–N), 886 (C–O) 660 (–Co–N). HRMS(m/e) Cal: 824.10 found: 824.4008.

X-ray structure

Monochromatic Ga K α radiation ($\lambda = 1.34139 \text{ \AA}$) was utilized in a Bruker D8 Venture diffractometer in order to generate X-ray crystal data. SHELXT [25] and SHELXL-2018/3 [26] were used to solve and revise the structures of complexes (I)-(III), respectively. OLEX2 [27] and MERCURY [28] were used to generate the molecular graphics. All atoms other than H were purified using anisotropic thermal parameters. Theoretical calculations were used to locate all the hydrogen atoms, which were subsequently adjusted using position parameters from the riding model and isotropic thermal settings. For a complete set of crystallographic data, see (Table 1).

| Complex | (I) | (II) | (III) |
|--|--|--|--|
| Empirical formula | ZnC ₁₆ H ₁₆ N ₆ O ₁₂ | CoC ₁₆ H ₁₆ N ₆ O ₁₂ | Ni ₂ C ₃₄ H ₃₈ N ₆ O ₁₁ |
| Formula mass | 549.72 | 543.28 | 824.10 |
| Temp (K) | 200.0 | 200.0 | 100(2) |
| Wavelength (Å) | 1.34139 | 1.34139 | 1.34139 |
| Crystal system | Monoclinic | Monoclinic | Triclinic |
| Space group | <i>P</i> 2 ₁ / <i>n</i> | <i>P</i> 2 ₁ / <i>n</i> | <i>P</i> -1 |
| <i>a</i> (Å) | 5.0921(4) | 5.0752(4) | 10.0957(3) |
| <i>b</i> (Å) | 15.3433(11) | 15.3303(13) | 12.5513(4) |
| <i>c</i> (Å) | 12.9483(9) | 12.9546(10) | 13.5639(4) |
| β (°) | 93.450(3)° | 92.839(3) | 85.4240(10) |
| Volume (Å ³) | 1009.81(13) | 1006.69(14) | 1702.15(9) |
| <i>Z</i> | 2 | 2 | 2 |
| <i>D</i> _{calcd} (g cm ⁻³) | 1.808 | 1.792 | 1.577 |
| μ (mm ⁻¹) | 1.603 | 5.168 | 6.419 |
| <i>F</i> (000) | 560 | 544 | 840 |
| θ range (°) | 5.015-61.564 | 3.889-60.385 | 2.843-72.462 |
| Total reflc. | 9459 | 12410 | 39900 |
| Unique reflections | 2324 | 2245 | 9855 |
| <i>R</i> _i , <i>wR</i> ₂ [<i>I</i> > 2 σ (<i>I</i>)] | 0.0436, 0.1199 | 0.0579, 0.1459 | 0.0355, 0.0941 |
| <i>R</i> _i , <i>wR</i> ₂ [all data] | 0.0488, 0.1236 | 0.0724, 0.1526 | 0.0432, 0.0968 |
| Residuals (e.Å ⁻³) | 0.487, -0.474 | 0.448, -0.627 | 0.389, -0.613 |

Table 1: Cell parameters and crystallographic data for complexes (I)–(III).

| D–H...A | <i>d</i> _{D–H} | <i>d</i> _{H...A} | <i>d</i> _{D...A} | \angle DHA |
|---------------------|-------------------------|---------------------------|---------------------------|--------------|
| For complex (I) | | | | |
| N(1)-H(1)...O(6)#2 | 0.88 | 1.99 | 2.778(3) | 148.3 |
| O(3)-H(3A)...O(2)#3 | 0.88 | 2.47 | 3.152(2) | 135.3 |
| O(3)-H(3A)...O(4) | 0.88 | 2.42 | 3.167(3) | 143.3 |
| N(2)-H(2)...O(4)#4 | 0.88 | 1.90 | 2.749(2) | 160.2 |
| For complex (II) | | | | |
| N(1)-H(1)...O(5)#2 | 0.88 | 1.96 | 2.763(4) | 150.9 |
| N(2)-H(2)...O(6) | 0.88 | 1.89 | 2.742(4) | 161.8 |

Symmetry codes: For (I), #1 = -*x* + 2, -*y* + 1, -*z* + 1, #2 = *x* + 3/2, -*y* + 1/2, *z* + 1/2; for (II), #1 = -*x*, -*y* + 1, -*z* + 1, #2 = *x* + 1/2, -*y* + 1/2, *z* + 1/2, #3 = *x* + 1, *y*, *z*, #4 = *x* - 1, *y*, *z*.

Results and discussion

Overview of the crystal structures for complexes (I)–(III)

Fig. 1 displays the stereogram and crystal structure of the complexes (I)–(III). Under specific experimental conditions, all the complexes from (I)–(III) crystallize in centrosymmetric space groups, i.e., *P*2₁/*n* for (I)/(II), and *P*-1 for (III) (Table 1). Complexes (I) and (II) are mononuclear metal complexes, which contain one complete neutral coordination molecule in

their asymmetric units. Complexes (III) is dinuclear metallic coordination compound. The asymmetric unit of complex (III), contains dinuclear Ni(II) coordination molecules and one half of DMF solvent. However, the apical positions of the two Ni(II) coordination are different. First, the axial positions were occupied by water molecule; second, the axial positions were furnished by each one water and DMF molecules.

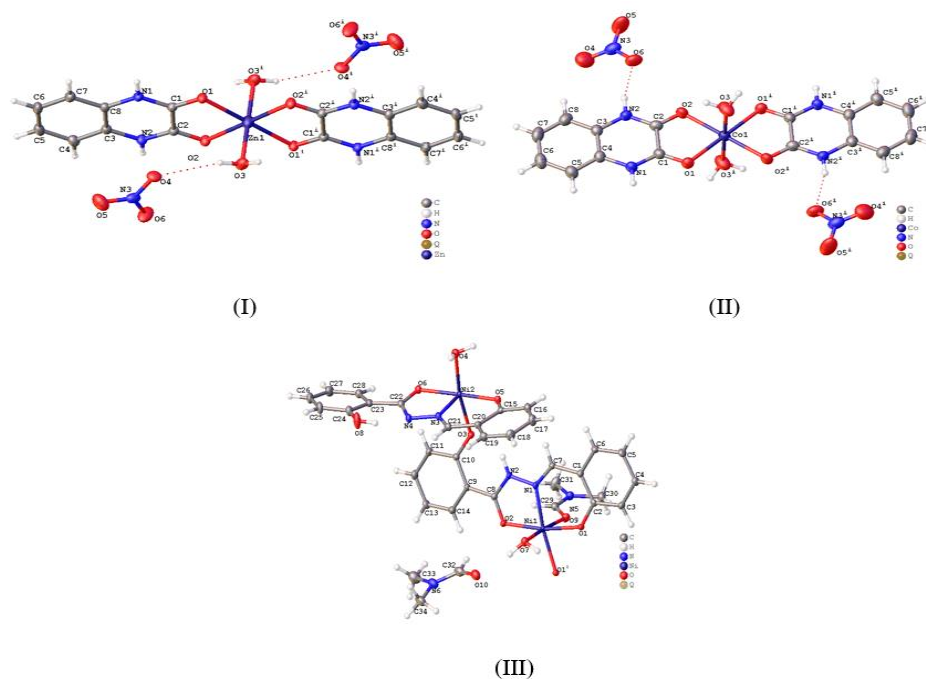


Figure 1: The ORTEP molecular structures of all three complexes, (I), (II), and (III), depicted as 30% thermal ellipsoid probability. In more detail, complex (I) contained a zinc ion, two 2,3 dihydroxyquinoxaline ligands, two nitrate ions, and two water molecules. Complex (II) contains one cobalt ion, two 2,3 dihydroxyquinoxaline ligands, two water molecules, and one nitrate ion. Both (complexes (I) and (II)) have a 5:1 ratio and octahedral geometry but have distinct center metal ions. Complex (III) contains two nickel ions, two salicylidene salicylhydrazide ligands, two DMF, and two water molecules.

In the crystal packing of complex (I), the coordination sphere of the central metal zinc ion adopted octahedral geometry by coordinating with four oxygen (O1, O2, O1ⁱ and O2ⁱ) from two 2,3 dihydroxyquinoxaline ligands and two water molecules coming with metal salt Zn(NO₃)₂·6H₂O. Both the water molecules are further connected with two nitrate ions (NO₃) via hydrogen bonding i.e. O(3)–H(3A)···O(4) and O(3ⁱ)–H(3Aⁱ)···O(4ⁱ) making complex (I). Each ligand has two nitrogen atoms (N1, N2 and N1ⁱ, N2ⁱ) inside the ring that do not take part in coordination with CMA which may be because of high bond distance from the center metal ion as well as the inter-delocalized bonding effect resonating hetero-cyclic alkenes rings. Both 2,3 dihydroxyquinoxaline ligands had strong electron-donating groups (-O), which were involved in coordination with zinc. The six bond lengths are $d_{Zn1-O2} = 2.0549(15)$ Å, $d_{Zn1-O2i} = 2.0549(15)$ Å, $d_{Zn1-O1} = 2.0990(15)$ Å, $d_{Zn1-O1i} = 2.0991(15)$ Å, $d_{Zn1-O3} = 2.1296(17)$ Å, and $d_{Zn1-O3i} = 2.1296(17)$ Å.

For the molecular structure of (II), the coordination sphere of the core metal cobalt ion took on an octahedral shape by combining with four oxygen (O1, O2, O1ⁱ, and O2ⁱ) from two 2,3 dihydroxyquinoxaline ligands and two water molecules resulting from the metal salt Co(NO₃)₂·6H₂O. Furthermore, each ligand has two nitrogen atoms (N1, N2 and N1ⁱ, N2ⁱ) inside the ring are not take part in coordination with CMA which may be because of the high bond distance from the center metal ion as well as the inter-delocalized bonding effect resonating hetero-cyclic alkenes rings, although forming hydrogen bonding with nitrate ions (NO₃⁻) i.e. N(2)–H(2)···O(6) and N(2ⁱ)–H(2ⁱ)···O(6ⁱ) in the coordination sphere of complex (II), this is just because of the symmetry operation which can be used to generate the omitted nitrate anion. The six bond lengths are $d_{Co1-O2} = 2.077(2)$

Å, $d_{Co1-O2i} = 2.077(2)$ Å, $d_{Co1-O3} = 2.091(3)$ Å, $d_{Co1-O3i} = 2.091(3)$ Å, $d_{Co1-O1} = 2.096(2)$ Å, and $d_{Co1-O1i} = 2.096(2)$ Å.

The dark green colored complex (III) is crystallized under a certain experimental condition, i.e., *P*-1. A di-nuclear nickel complex with two core nickel ions, two salicylidene salicylhydrazide ligands, two DMF, and two water molecules makes up the compound. It's interesting to observe that, both central nickel ions are not coupled to the same number of atoms. Octahedral geometry is formed by the connection of Ni1 to five oxygen (O1, O1ⁱ, O2, O7, O9) in which one oxygen each comes from water and DMF molecules, and one nitrogen atom (N1) from ligand. Furthermore, Ni2 is connected to four oxygens (O3, O4, O5, O6) in which O4 is coordinated from water while O3 is coming from the first ligand, and one nitrogen atom makes trigonal bipyramidal geometry. The six bond lengths for Ni (1) are $d_{Ni1-N1} = 1.9944(13)$ Å, $d_{Ni1-O1} = 1.9972(11)$ Å, $d_{Ni1-O1i} = 2.0324(11)$ Å, $d_{Ni1-O2} = 2.0487(11)$ Å, $d_{Ni1-O7} = 2.0873(12)$ Å, and $d_{Ni1-O9} = 2.1121(12)$ Å. For Ni (2), the five bond lengths are $d_{Ni2-N3} = 1.9691(14)$ Å, $d_{Ni2-O5} = 2.0386(11)$ Å, $d_{Ni2-O6} = 2.0411(11)$ Å, $d_{Ni2-O3} = 2.0925(11)$ Å and $d_{Ni2-O4} = 2.2049(12)$ Å.

IR analysis of complexes (I)-(III)

Several peaks were in the IR analysis that occur in all IR spectra (Fig. 2). Typically, infrared spectroscopy reveals that the vibrations of O–H groups are more affected by the surrounding environment. Consequently, the O–H group displayed an atypical infrared absorption peak. Generally, when there is no hydrogen bonding occurs between the free O–H groups, the O–H stretching vibrations typically produce strong absorption peaks with peaks in the 3750–3000 cm⁻¹ range. An OH (hydroxyl groups) was observed in our investigated compounds (III) for the infrared absorption vibration peak at 3728 cm⁻¹.

Additionally, the peak produced by the stretching vibrations of N–H groups falls between 3500–3100 cm⁻¹. This can be seen in all three complexes from 3370–3221 cm⁻¹. Since the stretching vibrations of the C=C bonds in the rings were observed by the absorption peaks from 1601 and 1664 cm⁻¹, the presence of aromatic structures was confirmed. The absorption peaks for C–

N, C–O, and C–C vibrations were found in complexes (I)–(III) at 1403 to 886 cm⁻¹. There are stretching vibration peaks at 647 cm⁻¹, 622 cm⁻¹, 660 cm⁻¹, and 590 cm⁻¹ for Zn–O, Co–O, Ni–N, and Ni–O, [29], respectively, that exemplifies the connection between metal and ligand interactions (Fig. 2).

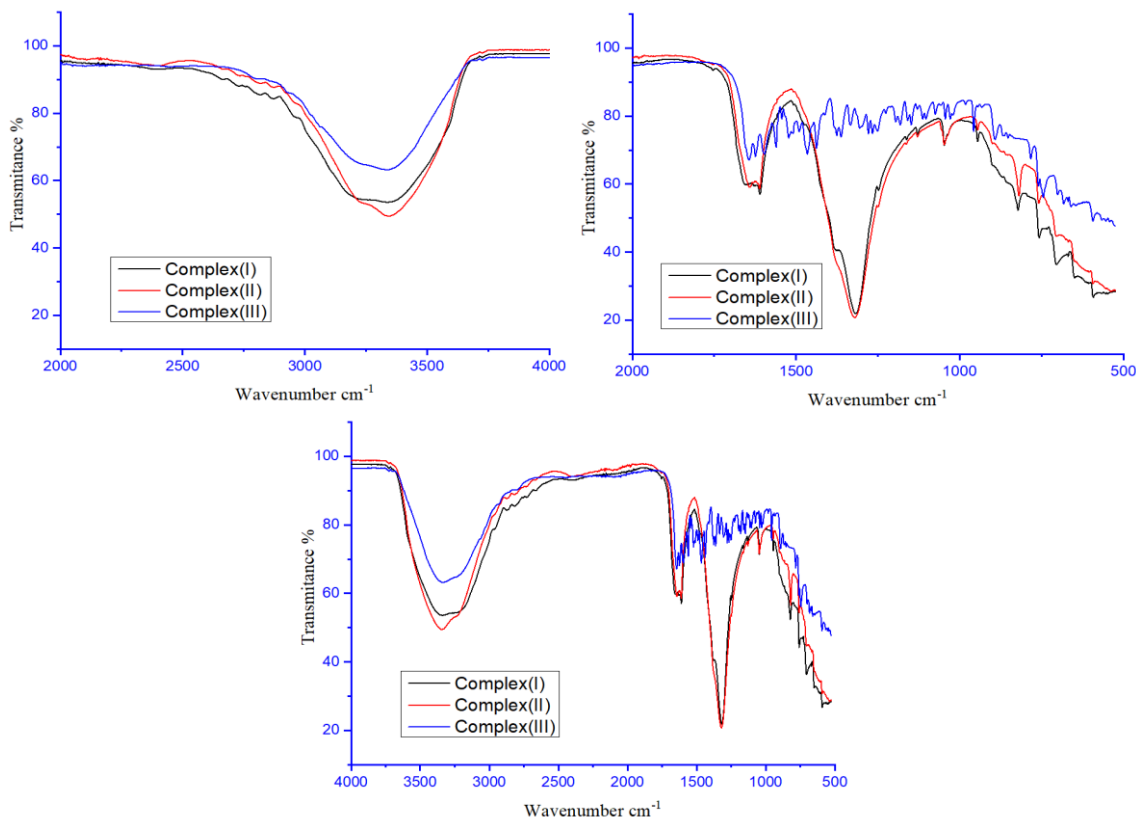


Figure 2: FTIR spectra of complexes (I)–(III)

UV–vis spectral analysis of complexes (I)–(III)

The coordination complex exhibits vibrant colours as a result of the presence of vacant d orbitals, which undergo d-d transitions upon interaction with light. This process leads to the absorption of specific wavelengths of light, resulting in complimentary colours being observed. The synthesized complexes were also characterized via UV–Vis (200–800 nm) because of their d-d transition and different peaks as compared to those of the raw material. All the complexes were dissolved in methanol and their characteristic peaks were analyzed [30,31]. The shift of lower to higher d-d transitions in the complexes that were absent from the ligand was due to the high electron density provided by

the ligands and d-d transitions (Fig 3). Complexes (I/II) produced a sharp peak at 250–380 nm while complex (III) at 210–240 nm and 300–325 nm had an absorption peak. This could be caused by the n→σ* transition of the C–O/C–N groups in the complex or by the n→π* transition of the C=O group. Perhaps, the central metal of complex (III) is Ni²⁺, which is green and has a strong absorbance, A broad and wide peak from ultraviolet to visible region 373–438 nm is because of the d-d transition in complex (III) for C=C, C–O Transition. For complexes (II), the central Co²⁺ which forms a brownish colour complex, having small absorption peaks at 460–540 nm.

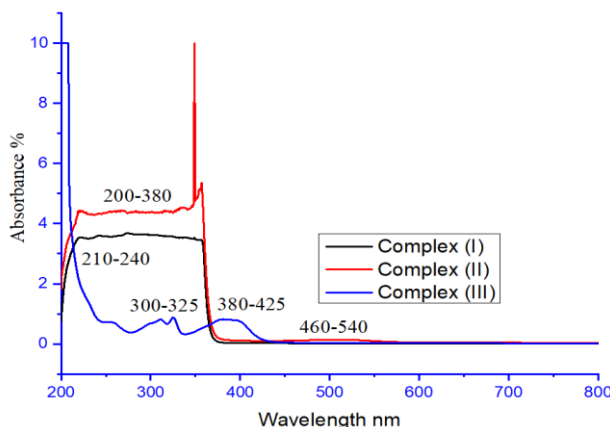


Figure 3: UV–vis spectra of complexes (I)–(III) in the range 200–800 nm.

Cytotoxicity assays of complexes (I)-(III)

The anticancer activity of complexes (I)–(III) and cisplatin were assessed, and the values of each compound were calculated using Reed and Muench's method [32], which demonstrated cytotoxic activity towards a variety of human cancer cell lines (SMMC-7721, A549, MDA-MB-231, and SW480). Complex (III) was the most effective, with an IC₅₀ value of 6.57 μM, against the human tumor cell line MDA-MB-231.

In pursuit of understanding the correlations between the structure and activity of the metal complexes under investigation, the physical and chemical characteristics of the ligands and metal ions were taken into account throughout the research process. Structurally, we found that the reported activities were linked to the central ions of the metal coordination spheres, the features and coordination modes of the ligands, and the properties of the auxiliary ligands [33,34].

It was found that Complex (II) exerted the least cytotoxic effect on all the cell lines. On the other hand, complex (III) (8.90 μM) and (I) (35.77 μM) were comparatively more cytotoxic to the

SMMC-7721 cell line. Similarly, Complex (III) (6.57 μM) was preferable to the other two complexes for its ability to treat the cell line MDA-MB-231. The best activity for cell lines SW480 and A549 was also shown by Complex (III) which are 10.16 μM and 19.3 μM, respectively. These findings led us to conclude that complex (III) produced the most potent cytotoxic effects against the four cancer cell lines (SMMC-7721, A549, MDA-MB-231, and SW480). Despite a high structural similarity of compounds (I) and (II), the anticancer activity of the compound (I) is more effective than that of compound (II), which indicates that the metal zinc ions are more beneficial in improving its anticancer activity. The relatively better activity of complex (III) compared to complexes (I and II) is likely attributed to the presence of coordinated DMF and water molecules, which can readily dissociate from the core metal and Ni(II) ion. This could enhance the interaction between metal ions and cancer cells. The ligands generated from organic hydrazides in complex (III) may also have a certain anticancer activity. In our laboratory, we are currently investigating other connections between the coordination environment of a metal atom and how it behaves.

| Complex | SMMC-7721 | SW480 | MDA-MB-231 | A549 |
|---------|---------------------|-------|------------|-------|
| | Cell Inhibition (%) | | | |
| I | 99.01 | 90.62 | 8.98 | 9.06 |
| II | 39.80 | 14.81 | 1.84 | 1.64 |
| III | 98.67 | 76.36 | 84.91 | 92.07 |

Table 3: Cell Inhibition (%) of complexes (I)-(III) to the different human tumor cell lines.

| Complex | SMMC-7721 | SW480 | MDA-MB-231 | A549 |
|---------|------------------------------------|-------|------------|------|
| | IC ₅₀ (μM) ^a | | | |
| I | 35.77 | 47.88 | --- | --- |
| II | --- | --- | --- | --- |
| III | 8.90 | 10.16 | 6.57 | 19.3 |
| cis | 16.90 | 15.30 | 18.01 | 8.49 |

Table 4: Cytotoxicities of complexes (I)-(III) to the different human tumor cell lines.

^aEach cell line's cytotoxicity was reported as an IC₅₀ value using the SRB assay; this value represents the concentration of the complex that resulted in a 50% reduction in cell number when compared to untreated cells. The drug cisplatin served as a control in these studies.

Conclusion

In conclusion, the crystal structures of two mononuclear (Zn(II) and Co(II)) **I–II** and one binuclear Ni(II) complex **III** were reported using a simple method and were employed in contradiction of different human tumor cell lines. All complexes crystallized in the chiral space groups (*P*₂₁/*n* for (I)/(II) and *P*–1 for (III)). Currently, research is underway on these complexes in various chemical processes, such as the coupling of amides with olefins and aldehydes.

Disclosure

Author Contributions: M. Luo designed the research and revised the article; Amir Nazeer performed the experiments, analysed the data, and wrote the manuscript; Qasim Umar helped in experiments and also performed the research work; Zhang Li and Yanting Yang also performed the research work; all the authors read and approved the final manuscript.

Data Availability Statement

Accession codes: complete crystallographic information files for all compounds have been deposited with the Cambridge Crystallographic Data Center as supplementary publications CCDC 2341288 (complex 1), 2341289 (complex 2) and 2341293 (complex 3). These data can be obtained free of charge via http://www.ccdc.cam.ac.uk/data_request/cif, by emailing data_request@ccdc.cam.ac.uk, or by contacting The Cambridge Crystallographic Data Centre, 12 Union Road, Cambridge CB2 1EZ, UK; fax: +44 1223 336033. Provided in the manuscript.

Supporting Information: Bond lengths and angles, crystal stacking, infrared data.

Acknowledgments: This work was supported by the Hefei University of Technology and State Key Laboratory of Photochemistry and Plant Resources in West China.

Declarations

Conflict of interest: The authors declare that they have no known competing financial interests or personal relationships that could have appeared to influence the work reported in this paper.

References

1. Frederick CA, Williams LD, Ughetto G, Van der Marel GA, Van Boom JH, et al. (1990) Structural comparison of anticancer drug-DNA complexes: adriamycin and daunomycin. *Biochemistry* 29: 2538-2549.
2. Vela L, Contel M, Palomera L, Azaceta G, Marzo I (2011) Iminophosphorane-organogold (III) complexes induce cell death through mitochondrial ROS production. *J Inorg Biochem* 105: 1306-1313.
3. Allardyce CS, Dyson PJ (2016) Metal-based drugs that break the rules. *Dalton Transactions* 45: 3201-3209.
4. Bredikhin AA, Gubaidullin AT, Bredikhina ZA, Fayzullin RR (2013) Crystallographic evidence of side-arm lariat effect in the series of chiral ortho - and para - methoxyphenoxymethyl-15-crown-5 complexes with sodium perchlorate. *J Mol Struct*. 1032: 176-184.
5. Glans L, Ehnbohm A, de Kock C, et al. (2012) Ruthenium (II) arene complexes with chelating chloroquine analogue ligands: synthesis, characterization and in vitro antimalarial activity. *Dalt Trans* 41:2764-2773.
6. Shivankar VS, Vaidya RB, Dharwadkar SR, Thakkar NV (2003) Synthesis, characterization, and biological activity of mixed ligand Co (II) complexes of 8-hydroxyquinoline and some amino acids. *Synth React Inorg Met Chem* 33: 1597-1622.
7. Huang S, Yang B, Luo S (2020) A theoretical study on spectroscopic properties and quantum yields of chiral-at-metal cyclometalated Pt (II) complexes. *J Mol Struct* 1199: 126975.
8. Sun B, Wang YC, Qian C, Chu, J, Liang SM et al. (2010) Synthesis, characterization and DNA-binding studies of chiral ruthenium (II) complexes with 2-(5-nitrofuranyl)-1H-imidazo [4, 5-f][1, 10] phenanthroline. *J Mol Struct* 963: 153-159.
9. Shiota N, Hige S, Kinuta T, Sato T, Kuroda R, et al. (2012) Preparation of a supramolecular heterocyclic host complex using chiral (1R, 2S)-2-amino-1, 2-diphenylethanol. *J Mol Struct* 1014: 32-37.
10. Paul MK, Kalita G, Laskar AR, Choudhury TD, Rao NVS (2013) Synthesis and mesomorphism of new chiral imines and copper (II) complexes. *J Mol Struct* 1039: 219-226.
11. Choksakulporn S, Punkvang A, Sritana-Anant Y (2015) Synthesis and amino acids complexation of tripodal hexasubstituted benzene chiral receptors. *J Mol Struct* 1082: 97-102.
12. Ma D lung, He H zhang, Leung K ho, Chan DS hin, Leung C hang (2013) Bioactive Luminescent Transition-Metal Complexes for Biomedical Applications. *Angewandte Chemie International Edition* 52: 7666-7682.
13. Pettinari C, Tăbăcaru A, Galli S (2016) Coordination polymers and metal-organic frameworks based on poly (pyrazole)-containing ligands. *Coord Chem Rev* 307: 1-31.
14. Lazreg F, Nagra F, Cazin CSJ (2015) Copper-NHC complexes in catalysis. *Coord Chem Rev* 293: 48-79.
15. Hu JM, Guo R, Liu YG, Cui GH (2016) Four Co (II) coordination polymers based on 4, 4'-bis (benzimidazol-1-ylmethyl) biphenyl and aromatic carboxylic acids co-ligands: Synthesis, structures, and photocatalytic properties. *Inorganica Chim Acta* 450: 418-425.
16. Abdolmaleki S, Panjehpour A, Khaksar S, Ghadermazi M, Rostamnia S (2023) Evaluation of central-metal effect on anticancer activity and mechanism of action of isostructural Cu (II) and Ni (II) complexes containing pyridine-2, 6-dicarboxylate. *Eur J Med Chem* 245: 114897.
17. Gangu KK, Maddila S, Mukkamala SB, Jonnalagadda SB (2017) Synthesis, characterisation and catalytic activity of 4, 5-imidazolecarboxylate ligated Co (II) and Cd (II) metal-organic coordination complexes. *J Mol Struct* 1143: 153-162.
18. Swamy G, Sivanarayanan P, Sridhar B, Joshi LR (2016) Crystal structure studies and antimicrobial activities of transition metal complexes of pyridine-2, 6-dicarboxylic acid and imidazole containing water clusters. *J Coord Chem* 69: 1602-1617.
19. Nfor EN, Keenan LL, Nenwa J, Ndifon PT, Njong RN, et al. (2014) A novel mixed ligand dinuclear complex of cobalt (II): synthesis, characterization and magnetic studies. *Cryst Struct Theory Appl*.
20. Salama MM, Ahmed SG, Hassan SS (2017) Synthesis, characterizations, biological, and molecular docking studies of some amino acid Schiff bases with their cobalt (II) complexes. *Adv Biol Chem* 7: 182.
21. Wang QB, Jing ZY, Hu XM, Lu WX, Wang P (2021) Synthesis, structure, and heterogeneous Fenton reaction of new Cu (ii)-based discrete Cu 2 L x coordination complexes. *CrystEngComm* 23: 216-220.
22. Pampa KJ, Karthik CS, Hema MK, Mallu P, Lokanath NK (2021) Post-synthetic modification of supramolecular assemblies of β-diketonato Cu (II) complexes: comparing and contrasting the molecular topology by crystal structure and quantum computational studies. *CrystEngComm* 23: 4344-4369.
23. Mardani Z, Kazemshoar-Duzdazani R, Moeini K, Hajabbas-Farshchi A, Carpenter-Warren, et al. (2018) Anticancer activities of a β-amino alcohol ligand and nanoparticles of its copper (II) and zinc (ii) complexes evaluated by experimental and theoretical methods. *RSC Adv* 8: 28810-28824.
24. Umar Q, Huang YH, Nazeer A, Zhang JC, Luo M, et al. (2022) Synthesis, characterization and anticancer activities of Zn 2+, Cu 2+, Co 2+ and Ni 2+ complexes involving chiral amino alcohols. *RSC Adv* 12: 32119-32128.
25. Sheldrick GM (2015) SHELXT-Integrated space-group and crystal-structure determination. *Acta Crystallogr Sect A Found Adv* 71: 3-8.
26. Yang Z, Cai X, Chen J, Shi Y, Huang P, et al. (2022) Sythesis, single crystal X-ray analysis, and DFT calculations of te rt-butyl 4-(4-nitrophenyl) piperazine-1-carboxylate. *Mol Cryst Liq Cryst* 738: 67-75.
27. Yamada T, Morikawa S, Kitagawa H (2010) Structures and proton conductivity of one-dimensional M(dhbq).nH 2O (M = Mg, Mn, Co, Ni, and Zn, H2(dhbq) = 2,5-dihydroxy-1,4-benzoquinone) promoted by connected hydrogen-bond networks with absorbed water. *Bull Chem Soc Jpn* 83: 42-48.
28. Saghatforoush LA, VALENCIAz L, CHALABIANx F, Ghammamy S, KHALEDIy LZ (2011) Synthesis, crystal structure, and biological activity of 4'-chloro-2,2': 6',2"-terpyridine (Cltpy) as tridentate ligand in a Cd(II) complex. *J Coord Chem* 64: 3311-3322.

29. Li Z, Yan H, Liu K, Huang X, Niu M (2019) Syntheses, structures, DNA/BSA binding and cytotoxic activity studies of chiral alcohol-amine Schiff base manganese (II/III) complexes. *J Mol Struct* 1195: 470-478.
30. Zeng C, Yang Y, Zhu Y, Wang H, Chu T, Ng SW (2012) A New Luminescent Terbium 4-methylsalicylate Complex as a Novel Sensor for Detecting the Purity of Methanol. *Photochem Photobiol* 88: 860-866.
31. Meng Q hong, Zhou P, Song F, Wang Y bing, Liu G lei, Li H (2013) Controlled fluorescent properties of Zn (II) salen-type complex based on ligand design. *CrystEngComm* 15: 2786-2790.
32. Błachut D, Wojtasiewicz K, Krawczyk K, Maurin J, Szawkało J, Czarnocki Z (2012) Identification and synthesis of by-products found in 4-methylthioamphetamine (4-MTA) produced by the Leuckart method. *Forensic Sci Int* 216: 108-120.
33. Wu H, Sun W, Shi T, Liao X, Zhao W, Yang X (2014) The various architectures and properties of a series of coordination polymers tuned by the central metals and auxiliary N-donor ligands. *CrystEngComm* 16: 11088-11095.
34. Zhang L, Luo M (2023) Synthesis and anticancer activities of Cu²⁺, Zn²⁺, Co²⁺ and Ni²⁺ complexes containing pyridine carboxylic acids. *J Clin Med Img Case Rep* 3: 1562.

Copyright: © 2024 Luo M. This Open Access Article is licensed under a [Creative Commons Attribution 4.0 International \(CC BY 4.0\)](https://creativecommons.org/licenses/by/4.0/), which permits unrestricted use, distribution, and reproduction in any medium, provided the original author and source are credited.